PERGAMON

Carbon 40 (2002) 437–444

CARBON

Ab initio molecular orbital study of adsorption of atomic hydrogen on graphite: Insight into hydrogen storage in carbon nanotubes

Frances H. Yang, Ralph T. Yang*

Department of Chemical Engineering, University of Michigan, 3074F H.H. Dow Building, 2300 Hayward Street, Ann Arbor, MI 48109, USA

Received 22 March 2001; accepted 24 June 2001

Abstract

Ab initio molecular orbital (MO) calculations are performed to study the adsorption of H atoms on three faces of graphite: (0001) basal plane, (1010) zigzag edge and (1121) armchair edge. The relative energies of adsorption (or C–H bond energies) follow the order: zigzag edge>armchair edge>basal-plane edge, in agreement with previous semi-empirical MO results. However, it is found that adsorption on the basal plane sites is exothermic and stable, in contrast to previous semi-empirical results. On the edge sites, the C–H bond energy decreases by nearly 30 kcal/mol when two H atoms are adsorbed on the same site. On the basal plane, the C–H bond energy decreases from 46 kcal/mol when two H are adsorbed on alternating sites to 27 kcal/mol when they are adsorbed on two adjacent sites. Literature MO results of H adsorption on the exterior wall of SWNT are in fair agreement with that on the basal plane of graphite. The value 27 kcal/mol agrees well with experiment (23 kcal/mol) of TPD of hydrogen from MWNT. Three common features exist in the reported experiments on hydrogen storage in carbon nanotubes: slow uptake, irreversibly adsorbed species, and the presence of reduced transition metals (Fe, Co or Ni). Combined with the MO results, a mechanism that involves H_2 dissociation (on metal catalyst) followed by H spillover and adsorption (on nanotubes) is proposed for hydrogen storage in carbon nanotubes.

Keywords: A. Graphite; Carbon nanotubes; C. Adsorption; Modeling; D. Adsorption properties

1. Introduction

The theoretical investigation on chemisorption of hydrogen on graphite has been of long-standing interest since the early quantum mechanical calculations of Sherman and Eyring [1]. Semi-empirical molecular orbital (MO) calculations have been used to understand the chemisorption of hydrogen on various planes of graphite [2–9]. The focus of these studies was on the adsorption on the basal plane (0001) of graphite. It was concluded that in the adsorption of H atoms on the basal plane, metastable states existed and the adsorption was endothermic [6–9]. Since more accurate ab initio methods are now available, the calculations are undertaken using these methods. From the results, insights into the current problem of hydrogen storage in carbon nanotubes are given.

Carbon nanotubes are formed by graphite (or graphene) sheets rolled up into tubes, generally in the range of 1–10 nm in diameter and 200–500 nm in length. The multiwall nanotubes (MWNT) were discovered by Iijima in 1991 [10]. Single-wall nanotubes (SWNT) were discovered in 1993 [11,12]. Since their discoveries, these materials have attracted intense interest due to their potential in applications in a variety of nanotechnologies [13–16], such as molecular electronics, scanning probe microscope tips (electron field emitters), quantum nanowires, catalyst supports, chemical sensors and sorbents for hydrogen storage. Our preliminary experimental results also showed that they are promising sorbents for selective adsorption of NO_x [17] and dioxins [18]. Beside MWNT and SWNT, carbon/graphite nanofibers (GNF) are closely related materials and have also shown a potential for hydrogen storage [19,20].

*Corresponding author. Tel.: +1-734-936-0771; fax: +1-734-763-0459.

E-mail address: yang@umich.edu (R.T. Yang).

0008-6223/02/$ – see front matter
PII: S0008-6223(01)00199-3

Much excitement has arisen from recent reports of promising results on carbon nanotubes for hydrogen storage [19–25]. High hydrogen adsorption capacities were reported for various carbon nanotubes. However, a good deal of controversy exists regarding reproducibility of the results. Dillon et al. [21] estimated that single-wall nanotubes could potentially store up to 5–10% by weight of hydrogen at 273 K based on temperature programmed desorption (TPD) data. From TPD, they determined that the activation energy for desorption of hydrogen from the nanotubes was 19.6 kJ/mol. This value is too high to be explained by physical adsorption. Chambers et al. [19], using a volumetric system, reported up to 67% by weight of hydrogen storage by platelet-GNF at 120 atm and 298 K. More recently, interesting results were reported on alkali-doped carbon nanotubes for hydrogen storage [22]. It was reported that Li- and K-doped carbon nanotubes adsorbed, respectively, 20 wt.% and 14 wt.% of hydrogen at 1 atm and mild temperatures (200 to 400°C for Li-doped and near room temperature for K-doped nanotubes). Unfortunately, most of the uptake was found to be due to moisture in the hydrogen that formed alkali hydroxides [23]. Most recently, Liu et al. [24] reported about 4–5% by weight of hydrogen adsorption in single-wall nanotubes, at 100 atm and room temperature. Adsorption of hydrogen on SWNT at 80 K was measured by Ye et al. [25]. A H/C ratio of about 1 was reported for hydrogen on crystalline ropes of SWNTs at 80 K and pressures >12 MPa [25]. The H_2 adsorbed on nanotubes was reported to undergo a rapid *ortho–para* conversion at 25 K [26]. It should be noted that the edge sites of graphite may play a significant role in H_2 storage, as they are abundant in GNF [19] as well as nanotubes after acid treatments and heat treatments [27] which are typically done in all experiments for sample purification and activation. Hence it is important to study edge sites in this work.

Theoretical studies of physical adsorption of H_2 on carbon nanotubes using Monte Carlo simulations have been performed by several groups [28–38]. Various fluid–fluid and fluid–solid interaction potentials have been used. However, none could account for or nearly account for the reported experimental data. For example, the target of 6.5 wt.% H_2 uptake at ambient temperature could not be achieved even by tripling the fluid–wall interaction potential [31]. Clearly other explanations are needed in order to account for any of the reported experimental results.

One common feature that exists in all reported experimental results, whether at ambient temperature or at cryogenic temperatures, is the *slow* uptake of H_2. In all cases, the uptakes were slow, and equilibria were reached after a time span of the order of hours. Meanwhile, the adsorbed hydrogen could not be desorbed completely in vacuo. For example, 21–25% of the adsorbed hydrogen remained and had to be desorbed at 473 K in vacuo [24]. Both results are clear indications of chemisorption. Since metals were contained in the nanotubes in all cases, dissociation of hydrogen to atomic H was likely to have occurred. In addition, hydrogen dissociation is known to take place on the edge sites of graphite with a free sp^2 electron per carbon site (e.g. Ref. [8]), although the process would be slow at ambient temperature. Consequently, hydrogen dissociation followed by spillover and chemisorption on the surface of nanotubes is an entire possibility [39,40]. Our experimental results on hydrogen storage on carbon nanotubes with various metal dopants will be published elsewhere [41]. From TPD, the activation energy for desorption from $NiMgO_x$/MWNT was 23 kcal/mol [41]. In this work, we report ab initio results on adsorption of H atoms on different planes of graphite.

2. Computational details

Theoretical studies on the chemisorption of atomic hydrogen on graphite have been reported in previous work [2–9] using semi-empirical molecular orbital (MO) calculations. In this work, the Gaussian 94 program [42] in the Cerius2 molecular modeling software [43] from Molecular Simulation, Inc. was used for all calculations in the ab initio MO study of the hydrogen–graphite system. The structures of two types of graphite models are shown in Fig. 1: model A has an unsaturated armchair edge on top and model B has an unsaturated zigzag edge; the other unsaturated boundaries for both models A and B are terminated with hydrogen. Studies of Chen and Yang [44,45] documented that such molecular systems were determined to be the most suitable models for graphite structures, since they yield parameters in excellent agreement with the experimental data.

Chemisorption of hydrogen atoms on both edge planes and basal planes of models A and B, as illustrated by models C, D, E and F in Fig. 2, were calculated as follows. The unrestricted Hartree–Fock (UHF) method with the basis set of 3-21G(d) was used for geometric optimization and the self-consistent field (SCF) energy of the optimized system, whereas the higher level, B3LYP/6-31G(d) was used for the single point energy and bond population calculations when more accurate results were required. The spin multiplicity of each calculation was determined using the method of Kyotani and Tomita [46]: the selected spin multiplicity resulted in a reasonable chemical structure, with the least spin contamination and the lowest energy state.

The geometry-optimized structures were used to calculate the energy of chemisorption (E_{ads}) according to the following expression:

$$E_{ads} = E_{graphite-hydrogen} - E_{graphite} - E_{hydrogen}$$

where $E_{graphite-hydrogen}$ is the SCF energy of the optimized hydrogen–graphite structure, $E_{graphite}$ is the SCF energy of an optimized graphite structure and $E_{hydrogen}$ is the SCF

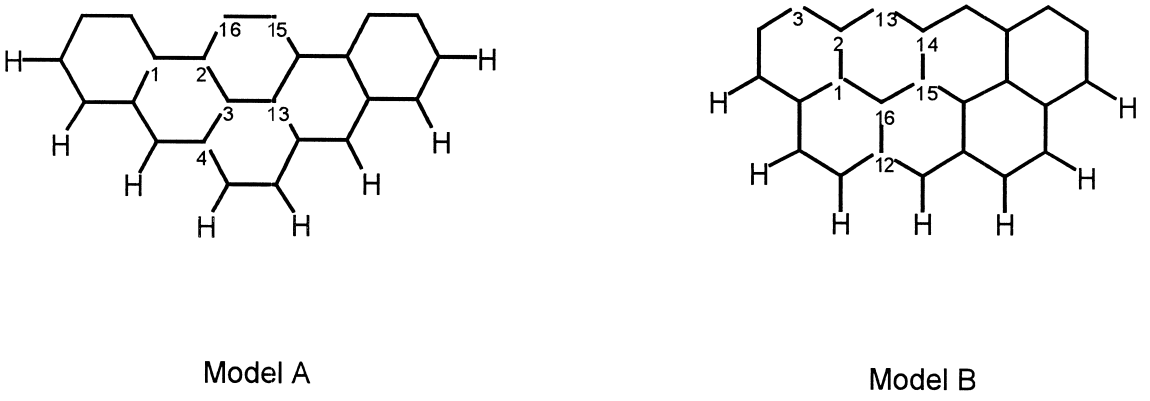

Fig. 1. Graphite models A and B.

energy of a hydrogen atom. The calculation was also applied to cases with two H atoms on each carbon site. A higher negative value of E_{ads} in kcal/mol corresponds to a stronger adsorption.

In order to determine the potential energy curves for the interaction between H atoms and graphite models, after geometry optimization of each molecular system, single point energy (SPE) was calculated upon each change of

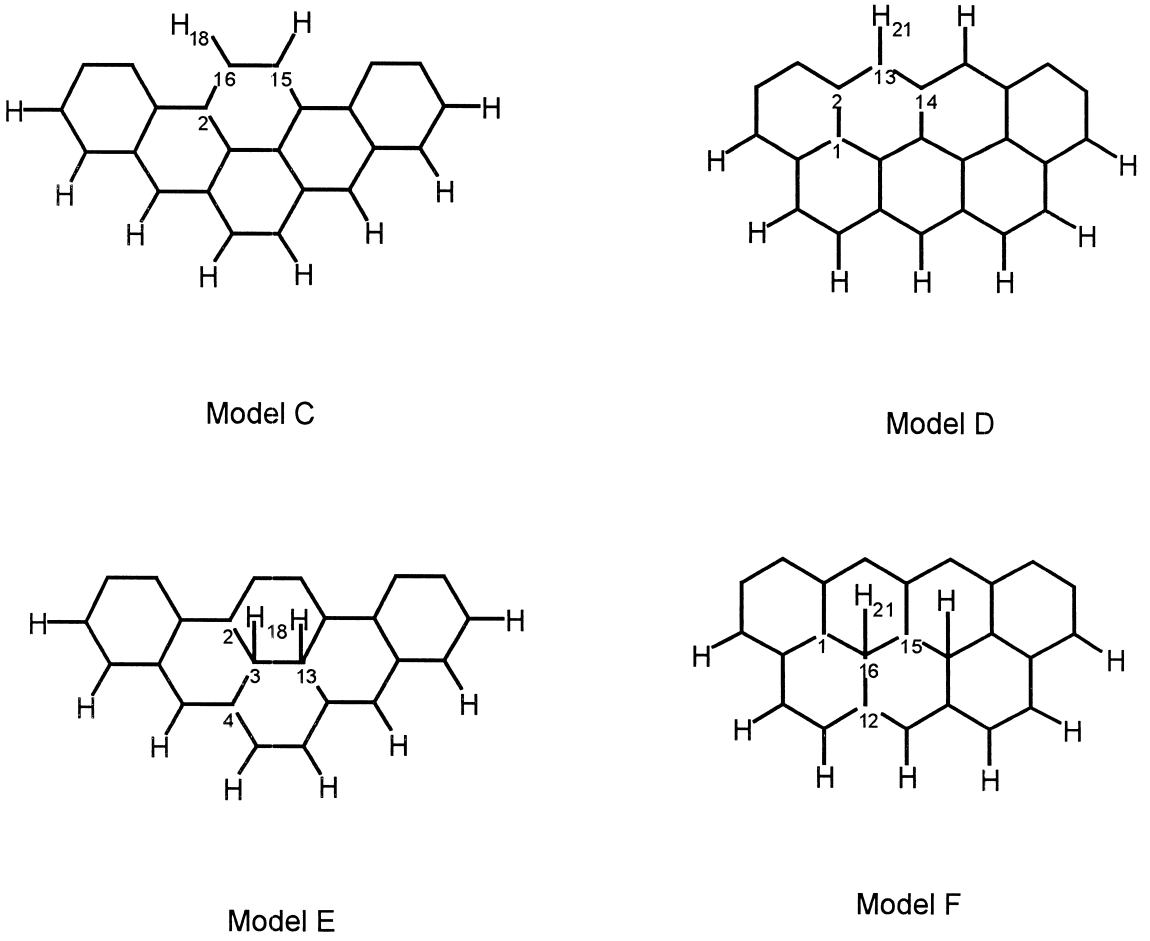

Fig. 2. Chemisorbed H on graphite models C, D, E and F.

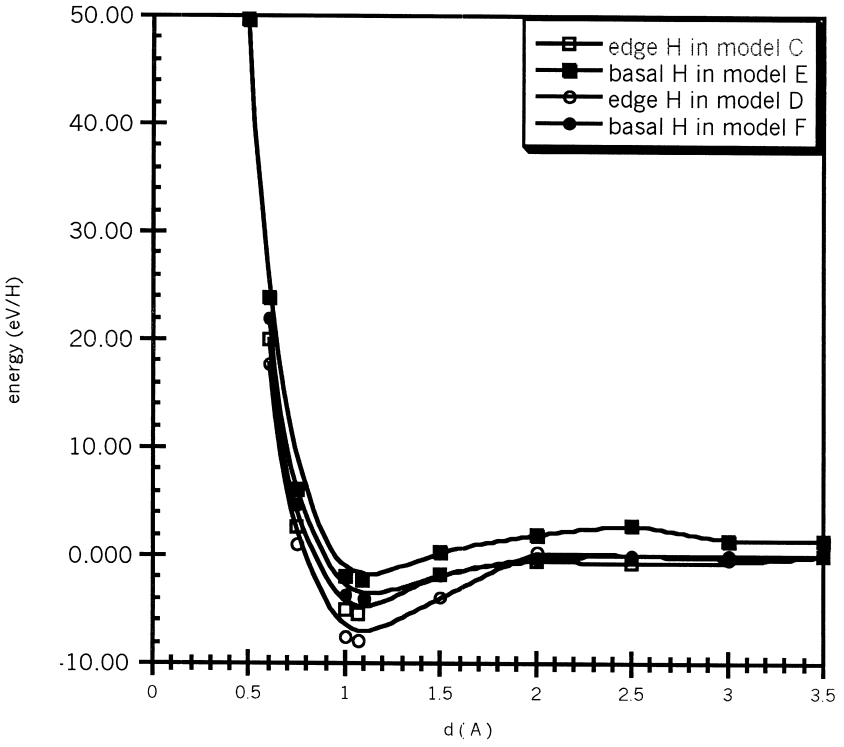

Fig. 3. Potential energy diagram for atomic H on models C, D, E and F.

the carbon–hydrogen bond length, and the resulting SPEs were converted to electron volt per hydrogen (eV/H) as presented in Fig. 3.

3. Results and discussion

3.1. Ab initio molecular orbital calculations on graphite models A and B

The values of the calculated bond lengths and bond angles for the optimized structures are in good agreement with the experimentally observed data [8]; the average bond lengths and bond angles are summarized in Table 1.

Table 1
Average bond length and bond angle for models A and B

	Model A	Model B	Exp. data
Avg. bond length (pm)			
C–C	142	141	142
C–H	107	107	107
Avg. bond angle (deg)			
C–C–C	120	120	120
C–C–H	120	120	120

The dihedral angles are all either 0° or 180° indicating that the graphite models are in the expected single plane sheet structure.

Some pertinent bond lengths and atomic bond populations are listed in Table 2. The atomic bond populations are derived from Mulliken population analysis and are used as a measure of bond strength. Values of bond length

Table 2
Bond length and atomic bond population for models A and B

Model	Bond	Length (pm)	Bond population
A	C(1)–C(2)	140	0.34
	C(2)–C(3)	144	0.48
	C(3)–C(4)	143	0.39
	C(2)–C(16)	141	0.47
	C(16)–C(15)	132	0.77
	C(3)–C(13)	144	0.46
B	C(1)–C(2)	146	0.34
	C(2)–C(3)	141	0.37
	C(2)–C(13)	139	0.38
	C(1)–C(16)	143	0.40
	C(16)–C(12)	143	0.39
	C(16)–C(15)	143	0.41
	C(13)–C(14)	140	0.38

Table 3
Bond length and atomic bond population of H-graphite for models C and D

Model	Bond	Length (pm)	Bond population
C	C(1)–C(2)	144	0.39
	C(2)–C(3)	143	0.49
	C(3)–C(4)	144	0.41
	C(2)–C(16)	142	0.43
	C(16)–C(15)	138	0.54
	C(3)–C(13)	143	0.43
	C(16)–H(18)	107	0.40
D	C(1)–C(2)	144	0.37
	C(2)–C(3)	141	0.34
	C(2)–C(13)	141	0.40
	C(1)–C(16)	142	0.41
	C(16)–C(12)	143	0.39
	C(16)–C(15)	142	0.40
	C(13)–C(14)	140	0.40
	C(13)–H(21)	107	0.40

and bond populations are used to compare to those of the hydrogen–graphite systems in Tables 3 and 4.

3.2. Chemisorption of H atom on the graphite edge sites

In Fig. 2, model C represents the structure of one hydrogen atom chemisorbed per edge carbon on the armchair plane of graphite, and model D represents the structure of one hydrogen atom chemisorbed per edge carbon on the zigzag edge of graphite. As indicated in Table 3, upon chemisorption of hydrogen on the edge sites, except for C(16)–C(15), no significant changes are noted in bond length or bond population for both zigzag and armchair edges. Also the dihedral angles are all unchanged, i.e. they are either 0° or 180°, indicating the structures remain as flat sheets. For C(15) and C(16), both bonded with H, the C–C bond is substantially weakened by H adsorption (the bond population decreases from 0.77 to 0.54) and the bond length is increased from 132 to 138 pm.

Table 4
Bond length and atomic bond population of H-graphite for models E and F

Model	Bond	Length (pm)	Bond population
E	C(1)–C(2)	143	0.34
	C(2)–C(3)	155	0.27
	C(3)–C(4)	152	0.26
	C(2)–C(16)	138	0.42
	C(16)–C(15)	133	0.44
	C(3)–C(13)	159	0.27
	C(3)–H(18)	109	0.41
F	C(1)–C(2)	143	0.36
	C(2)–C(3)	141	0.38
	C(2)–C(13)	141	0.35
	C(1)–C(16)	153	0.28
	C(16)–C(12)	152	0.27
	C(16)–C(15)	151	0.29
	C(13)–C(14)	141	0.36
	C(16)–H(21)	110	0.39

3.3. Chemisorption of H atom on the graphite basal plane sites

In Fig. 2, models E and F represent hydrogen atoms adsorbed on the basal plane sites. In model E, two hydrogen atoms are bonded to two adjacent carbons, and in model F they are further apart, with one carbon in between. In both cases, there are some significant increases in C–C and C–H bond lengths where hydrogen is directly involved, and decreases in bond population, indicating weaker C–C and C–H bonds, as shown in Table 4. The dihedral angles are no longer 0° or 180°, they deviate from 1° to 5°, so that the single layer sheet appears to curve away slightly from hydrogen.

Semi-empirical calculations [5–8] have all shown that adsorption of H atom on the basal plane is metastable and endothermic, because the potential energy diagram is always positive. The ab initio results from this work show that the previous results are not accurate, and in fact, the opposite conclusion is reached; the adsorption is exothermic and stable. The potential energy curves are shown in Fig. 3. This result has ramifications on hydrogen storage in carbon nanotubes, as will be discussed shortly.

3.4. Chemisorption of 2 H atoms per carbon on the graphite edge sites

In Fig. 4, model G represents the structure of two hydrogen atoms chemisorbed per edge carbon of the armchair face of graphite, and model H represents the structure of two hydrogen atoms chemisorbed per edge carbon of the zigzag face. Table 5 shows the bond lengths and bond populations of these two systems. Similar to the chemisorption of one H atom per edge C, the C–C bonds are weakened where H atoms are directly involved. The extent of C–C bond weakening is significantly higher with 2 H atoms bonded on each C. Also, the C–H bond is weaker when 2 H atoms are bonded to one carbon. All the dihedral angles remain unchanged, i.e. 0° or 180°, indicating the graphite systems remain as flat sheets. The bond angle formed between the two H atoms for both G and H, i.e. H–C–H is close to 107°.

Gaussian calculations for geometric optimization of graphite systems with 3 H atoms per carbon chemisorbed on the edge graphite sites or 2 H atoms per carbon on the basal graphite sites were attempted but ended in error terminations, this may be due to the limited tetravalent nature of the carbon atom. Our earlier semi-empirical MO

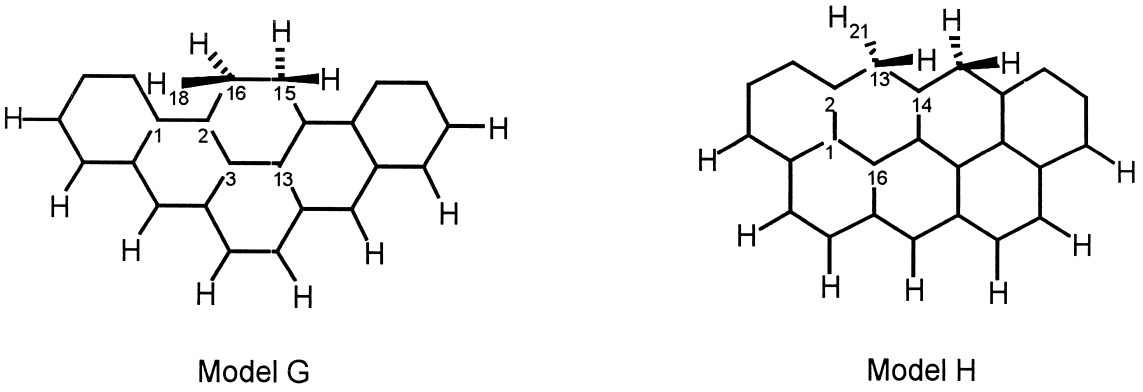

Fig. 4. Chemisorption of 2 Hs on models G and H.

Table 5
Bond length and atomic bond population of H-graphite for models G and H

Model	Bond	Length (pm)	Bond population
G	C(1)–C(2)	142	0.42
	C(2)–C(16)	152	0.23
	C(16)–C(15)	155	0.25
	C(3)–C(13)	148	0.36
	C(16)–H(18)	108	0.40
H	C(1)–C(2)	143	0.37
	C(2)–C(13)	151	0.26
	C(13)–C(14)	151	0.28
	C(1)–C(16)	143	0.40
	C(13)–H(21)	109	0.39

results indicated that the C–C bond on the edges would break when 3 H atoms are bonded to each C [9].

3.5. Heats of adsorption or bond energies

In Table 6, the energy of chemisorption E_{ads} is tabulated for each of the H-graphite systems. Values for C and D are similar to the reported C–H bond energies by semi-empirical MO calculations in our previous work [8,9]. However, considerable adjustments based on empiricism were needed in those energy calculations. In the present study with ab initio MO calculations, no empirical adjustments are needed, and it is found that both edge planes and basal planes in graphite can chemisorb hydrogen. The strength of chemisorption is higher on the edge planes than the basal planes, and follows the order:

zigzag edge > armchair edge > basal-plane.

Table 6
Calculated E_{ads} per H atom for models C, D, E, F, G and H

Model	E_{ads} (kcal/mol)
C (H on armchair edge)	−85.27
D (H on zigzag edge)	−90.24
E (H adjacent basal sites)	−27.04
F (H on alternating basal sites)	−46.47
G (2 H on armchair edge)	−56.93
H (2 H on zigzag edge)	−64.51

The potential energy curves in Fig. 3 also show that chemisorption on basal planes follows that same pattern as edge planes, with edge planes more stable than basal planes.

Two conclusions become clear from the results shown in Table 6. For adsorption on both edge planes, the bond energy (or energy of adsorption) decreases precipitously when two H atoms are adsorbed on each carbon site as compared with one H per site. In both cases, a nearly 30 kcal/mol decrease is seen. For adsorption on the basal plane sites, the energy of adsorption is substantially lower when the H atoms are occupying adjacent sites. Comparing model F with model E, the energy drops from 46.47 kcal/mol (two H on alternate sites) to 27.04 kcal/mol (two H on adjacent sites). This result also has implications on hydrogen storage in nanotubes as discussed below.

3.6. Comparison between graphite and nanotube

Interesting molecular orbital calculations have been published recently on the bonding of F atoms [47,48] and H atoms [49–51] on SWNT. The results on H-SWNT will be compared with our results.

Both Bauschlicher [49,50] and Froudakis [51] studied the bonding of H atoms on the *exterior* wall of the SWNT (both consisting of 200 C atoms, but with different diameters). Bauschlicher calculated the bond energies for the tube with 1 H, 2 H, 24% coverage, 50% and 100% coverages (assuming 1 H/1 C). The average C–H bond energy for the first H was 21.6 kcal/mol, and 40.6 kcal/mol for the first two H atoms. The average bond energy for 50% coverage was 57.3 kcal/mol, decreasing to 38.6

kcal/mol for 100% coverage. Froudakis studied the bonding of 1 H with the tube where the H atom approached the tube wall in two ways: direct approach to the top of a carbon atom, and approach along the centerline of a hexagon [51]. The energy minima were, respectively, 21 kcal/mol and 56 kcal/mol. Froudakis also reported the C–C bond lengths in the nanotube after H bonding. With 16 H bonded to 64 C on the 200-atom tube, the C–C bond length increased from 143 to 159 pm [51].

The C–H bond energies on the tube are in general agreement with that on the basal plane of graphite. The energies on the basal plane are 46.47 kcal/mol for two alternating or separated H atoms, and 27.04 kcal/mol for two adjacent H atoms. A similar crowding effect was also seen on the curved tube, i.e. 57.3 kcal/mol for 50% coverage and 38.6 kcal/mol for 100% coverage [50]. The increase in the C–C bond lengths from 143 to 155–159 pm by adsorption of H was also seen on the basal plane of graphite, and are, in fact, in excellent agreement with our results (Tables 4 and 5).

From the above comparison, it is unlikely that the adsorption of H atoms would be significantly different on the basal plane of graphite and on the exterior wall of the nanotube. No calculation results have appeared in the literature on H adsorption on the interior surface of the tube. Based on the results above, it is possible that the binding energies could be further lowered for adsorption inside the tube.

3.7. Inference on hydrogen storage in nanotubes

As mentioned in the Introduction, there existed a number of common features in all the experimental reports on hydrogen storage in carbon nanotubes. Firstly, the adsorption was slow, lasting for a time span of the order of hours. Secondly, the stored hydrogen could not be desorbed completely at ambient temperature in vacuo; a substantial fraction could be desorbed only at substantially higher temperatures. Thirdly, whether the nanotubes were formed by arc discharge (where Co or Co plus other metals were used) or by catalytic hydrocarbon decomposition (where Fe, Ni and other metals were used), transition metals (Fe, Co or Ni) were present and were mixed intimately with the carbon nanotubes. In addition, the samples were subjected to heat treatments prior to measurements of hydrogen storage. For example, MWNTs mixed with $Ni_{0.4}Mg_{0.6}O$ catalyst were treated at 500°C in our own work [23]. In our case, the heat treatment was carried out in H_2, although in some of the other cases the heat treatments were done in vacuo or in an inert atmosphere. In all cases, however, the surfaces of the transition metals were undoubtedly reduced (on the carbon support). These reduced metal surfaces are excellent catalysts for hydrogen dissociation, at temperatures near room temperature.

These common features point to the possibility or likelihood of hydrogen storage that follows the mechanism of H_2 dissociation with subsequent H spillover and adsorption. Once H atoms are available, bonding to all three planes of graphite should follow, based on the MO results. Our results show that adsorption of H on the basal plane graphite sites is exothermic and stable, and is hence entirely feasible. The C–H bond energy decreases from 46 to 27 kcal/mol when two H atoms move from two alternate sites (model F) to two adjacent sites (model E). The value 27 kcal/mol is in good agreement with experimental data of 23 kcal/mol [41]. The surfaces on the inner walls of the nanotubes are curved. There is a possibility that the C–H bond energy on such curved surfaces can be further lowered. Obviously a distribution of energies would exist. The adsorption of 1 H per carbon would correspond to 8.3% wt. storage.

References

[1] Sherman A, Eyring H. J Am Chem Soc 1932;54:2661.
[2] Bennett AJ, McCarroll B, Messmer RP. Surf Sci 1971;24:191.
[3] Bennett AJ, McCarroll B, Messmer RP. Phys Rev B 1971;3:1397.
[4] Dovesi R, Pisani C, Ricca F, Roetti C. J Chem Phys 1976;65:3075.
[5] Dovesi R, Pisani C, Roetti C. Chem Phys Lett 1981;81:498.
[6] Illas F, Sanz F, Virgili J. J Mol Struct 1983;94:79.
[7] Barone V, Lelj F, Minichino C, Russo N, Toscano M. Surf Sci 1987;189–190:185.
[8] Chen JP, Yang RT. Surf Sci 1989;216:481.
[9] Pan ZJ, Yang RT. J Catal 1990;123:206.
[10] Iijima S. Nature 1991;354:56.
[11] Iijima S, Ichihashi T. Nature 1993;363:603.
[12] Bethune DS, Kiang CH, de Vries MS, Gorman G, Savoy R et al. Nature 1993;363:605.
[13] Dresselhaus MS, Dresselhaus G, Eklund PC. Science of fullerenes and nanotubes, New York: Academic Press, 1995.
[14] Ajayan PM. Prog Cryst Growth Charact 1997;34:37.
[15] Subramoney S. Novel nanocarbons — structure, properties, and potential applications. Adv Mater 1998;10:1157.
[16] Kong J, Franklin NR, Zhou C, Chapline MG, Peng S, Cho K, Dai H. Science 2000;287:622.
[17] Long RQ, Yang RT. Ind Eng Chem Res, (2001) in press.
[18] Long RQ, Yang RT. J Am Chem Soc 2001;123:2059.
[19] Dillon AC, Jones KM, Bekkedahl TA, Kiang CH, Bethune DS, Heben MJ. Nature 1997;386:377.
[20] Chambers A, Park C, Baker RTK, Rodriguez NM. J Phys Chem B 1998;102:4253.
[21] Park C, Anderson PE, Chambers A, Tan CD, Hidalgo R, Rodriquez NM. J Phys Chem B 1999;105:10372.
[22] Chen P, Wu X, Lin J, Tan KL. Science 1999;285:91.
[23] Yang RT. Carbon 2000;38:623.
[24] Liu C, Fan YY, Liu M, Cong HT, Cheng HM, Dresselhaus MS. Science 1999;286:1127.
[25] Ye Y, Ahn CC, Witham C, Fultz B, Liu J, Rinzler G et al. Appl Phys Lett 1999;74:2307.

[26] Brown CM, Yildirim T, Neumann DA, Heben MJ, Gennett T, Dillon AC et al. Chem Phys Lett 2000;329:311.
[27] Kuznetsova A, Mawhinney DB, Naumenko V, Yates Jr. JT, Liu J, Smalley RE. Chem Phys Lett 2000;321:292.
[28] Wang Q, Johnson JK. Mol Phys 1998;95:299.
[29] Wang Q, Johnson JK. J Chem Phys 1999;110:577.
[30] Wang Q, Johnson JK. J Phys Chem B 1999;103:277.
[31] Wang Q, Johnson JK. J Phys Chem B 1999;103:4809.
[32] Simonyan VV, Diep P, Johnson JK. J Chem Phys 1999;111:9778.
[33] Darkrim F, Levesque D. J Chem Phys 1998;109:4981.
[34] Rzepka M, Lamp P, de la Casa-Lillo MA. J Phys Chem B 1998;102:10894.
[35] Gordon PA, Saeger RB. Ind Eng Chem Res 1999;38:4647.
[36] Yin Y, McEnaney B, Mays T. Langmuir 2000;16:10521.
[37] Chen HS, Pez G, Kern G, Kress G, Hafner J. J Phys Chem B 2001;105:736.
[38] Claye AS, Fischer JE. Electrochem Acta 1999;45:107.
[39] Robell AJ, Ballou EV, Boudart M. J Phys Chem 1964;68:2748.
[40] Boudart M, Aldag AW, Vannice MA. J Catal 1970;18:46.
[41] Lueking AD, Yang RT. University of Michigan, in preparation.
[42] Frisch MJ, Trucks GW, Schlegel HB, Gill PMW, Johnson BG, Robs MA et al. Gaussian 94, revision B.3, Pittsburgh, PA: Gaussian Inc, 1995.
[43] Bowie JE. Data visualization in molecular science: tools for insight and innovation, Reading, MA: Addison-Wesley, 1995.
[44] Chen N, Yang RT. Carbon 1998;36:1061.
[45] Chen N, Yang RT. J Phys Chem A 1998;102:6348.
[46] Kyotani T, Tomita A. J Phys Chem B 1999;103:3434.
[47] Seifert G, Kohler T, Frauenheim T. Appl Phys Lett 2000;77:1313.
[48] Kudin KN, Bettinger HF, Scuseria GE. Phys Rev B 2001;63:45413.
[49] Bauschlicher Jr. CW. Chem Phys Lett 2000;322:237.
[50] Bauschlicher Jr. CW. Nano Lett 2001;1:223.
[51] Froudakis GE. Nano Lett 2001;1:179.